Journal of Ceramic Processing Research. Vol. 22, No. 1, pp. 98~105 (2021)
(Received 12 September 2020, Received in revised form 1 November 2020, Accepted 11 November 2020)
https://doi.org/10.36410/jcpr.2021.22.1.98

J O U R N A L O F
Ceramic Processing Research

Corrosion behaviour of hydroxyapatite coatings on AZ31 and AZ91 magnesium alloys by plasma spray

Serkan Baslayici[a,b], Mehmet Bugdayci[b,c] and Mahmut Ercan Acma[a]
[a]*Istanbul Technical University, Faculty of Chemistry & Metallurgy, Metallurgical and Materials Eng. Dep., 34469, Istanbul, Turkey*
[b]*Istanbul Medipol University, Vocational School, Construction Technology Dep., 34810, Istanbul, Turkey*
[c]*Yalova University, Faculty of Engineering, Department of Chemical Engineering, 77200, Yalova, Turkey*

In the scope of this study, AZ31 and AZ91 magnesium alloys are to be coated with hydroxyapatite by plasma spray to be used as biodegradable implant material and their in-vitro corrosion behaviors are to be examined. There are a number of researches on the production of biodegradable cortical screws and plates used in orthopedic surgery in last decade. The advantage of biodegradable implants is that they do not need to be surgically removed. Moreover, the elastic modulus and the mechanical properties of magnesium are relatively close to those of the human bone, and this prevents the phenomenon of the human bone named "stress shielding. During this study, the hydroxyapatite coating processes, characterizations and corrosion behaviors of AZ31 and AZ91 will be examined. The aim of this work is to determine the optimal coating conditions for magnesium alloys for biodegradable implants. As a result of the plasma spray coating, the corrosion rate has decreased from about 1.2 mm/year to 0.4 mm/year.

Keywords: Mg alloys, Hydroxyapatite, Biodegradable, Plasma spray, Ceramic coating.

Introduction

Titanium alloys, Co-Cr alloys and stainless steels are among the best choices as metallic bio-alloys for hard tissue replacement procedures due to some of their material properties. The mechanical properties, corrosion behavior, and bio-compatibility are the most important characteristics for these materials for this procedure [1, 2]. When these alloys are used in implants, a second surgery is necessary to remove these implants from bodies of patients. Therefore, development of bio-degradable materials especially for cardiovascular stents and hard tissue replacements is highly in demand in medical sector. This demand also exists in the area of ceramic based biomaterials and biopolymers. Neither ceramic based biomaterials nor the biopolymers can provide the necessary mechanical properties and bio-degradability for the aforementioned procedures like bio alloys [2, 3]. In the last decade, lots of research has been done in this area and iron (Fe), magnesium (Mg) and zinc (Zn) are chosen as candidate materials due to their biodegradability and nontoxicity properties. The reasons for the research of magnesium alloys as bio-materials are the biocompatibility and osteointegrity properties of magnesium. The problem with magnesium is that its corrosion rate in body is too high. For instance, the desired biodegrading period for cardiovascular stents is 12-24 months but this desired value is high for magnesium. For this reason, alloying of magnesium is considered as a valuable option to reduce its corrosion rate [1-7].

Metal ions released from biodegradable alloys can cause short term and long-term physiological reactions. The toxicity properties of a metallic material are not only related to its structure and its components' structure but also to its corrosion rate. In saline medium, magnesium-based alloys degrade to magnesium chlorides, magnesium oxides, magnesium sulfides and magnesium phosphates. It is stated in the literature that the ions released from magnesium alloys do not cause toxicity. Moreover, these ions are considered to have positive effects on certain tissues. Ideally, the use of potentially toxic elements in the design of biodegradable materials should be avoided. If this is not possible, these elements should be used within the acceptable limits and used as little as possible. Therefore, toxic elements should be determined, and these elements should not be used in next generation magnesium alloys. The most common alloying elements with magnesium are Al, Zn, Mn, Si, rare earth elements (RE), Zr, Ag and Y. Mg-1X binary alloys are prepared by adding Al, Ag, Mn, Si, Y, Zn and Zr 1% by weight elements separately and the reactions given by bones and veins to the ions of elements which are added to magnesium are evaluated [8-10].

Biodegradable implants act as intelligent implants and have gained more interest among the researchers in this area over the years. The main driving force behind the development of biodegradable implants is the

*Corresponding author:
Tel : +90(216)-681-56-66
E-mail: sbaslayici@medipol.edu.tr

degradability in the physiological environment. The properties of this class of materials are that they can be applied to the required area in the same way as permanent implants, but they can degrade in time without the need for a second surgery after healing has been completed. Lifelong problems with permanent implants also diminish due to this reason. Examples of these problems include endothelial dysfunction, permanent physical discomfort, and chronic local infections. Polymers in today's medical sector are mostly used, but Mg-based, Fe-based, and Zn-based alloys have been mentioned in the literature as better biodegradable materials due to their higher strength and ductility properties. As a biodegradable implant material, Mg based alloys have significant advantages over Fe and Zn based alloys. Research groups working on development of Fe-based and Zn-based biodegradable implant materials are very rare [11, 12]. Although Mg, Fe and Zn are important nutrients in healthy bodies, the daily amount of Mg should be in the range of 240-420 mg/day, the daily amount of Fe should be 8-18 mg/day, and the daily amount of Zn should be 8- 11 mg/day. This shows that the Daily amount of Mg needed in body is approximately 50 times more than Fe and Zn. A problem with pure Zn implants is that daily ingestion of 100-300 mg Zn can cause health problems and higher amounts can cause even greater problems. Young modulus of Mg (41-45 GPa) is closer to that of natural bone (3-20 GPa) than Fe (~ 211,4 GPa) and Zn (~ 90 GPa). If there is a large difference between the Young modules of the implant and the bone, there may be a problem named stress shielding. This biomedical incompatibility can lead to critical health problems such as early implant loosening, prolongation of the healing process, thinning of the bones, and chronic infections. It is mentioned in the literature that pure Fe and Zn are perfectly compatible with the human body and do not show local or general toxicity. Nevertheless, researchers have recently found that for biodegradable stents, iron corrosion products are a poor option because they accumulate as bulky speckle patterns on arterial walls of the living mouse over a period of 9 months. It has been found that when magnesium implants are used as internal fixator, they support the formation of new bone tissue. Investigating magnesium alloys as cardiovascular and orthopedic implants is not a new concept. The first clinical applications were made in 1878 by physiologist Edward C. Huse. Huse used magnesium wire to stop hemorrhages during the investigations. In his first studies, he found that magnesium was degrading too fast and was also very fragile. As a result, the use of magnesium and magnesium alloys as medical implants almost came to an end. The studies on magnesium as a biomaterial have been accelerated with the production of magnesium in high purity and high mechanical and corrosion performance as a result of technological developments. Heublein et al. made important studies on the cardiovascular stent by using this high degradability characteristic of magnesium in 2000-2003. Clinical tests have shown that magnesium stents do not show any allergic or toxic effects. It has also been shown that magnesium stents, like other permanent metallic stents, can give immediate angiographic results, but degrade fully in a period of 4 months. In the recent past, the first magnesium based orthopedic product, MAGNEZIX screw, has been introduced to the medical market and this product has been CE certified for use in medical applications in Europe. After this study, animal experiments were carried out for various applications of magnesium-based products. Although major studies have been made on magnesium based biodegradable implants in the last 15 years, some fundamental problems still cannot be solved. The high rates of corrosion of magnesium-based implants and the resulting loss in mechanical properties, especially in physiological environments at pH 7.4-7.6 (especially in high-chlorine environments) constitute a major problem [6, 13-15].

The implant material could be surface treated to enhance both the corrosion resistance and the biocompatibility. This method has practically been used in metal implants, such as stainless steel, titanium, and titanium alloys. For biomedical applications, various surface treatments have been adopted for Mg and its alloys in order to control the degradation rate and improve the biocompatibility [2, 16, 17]. In the literature, the electrochemical and immersion test results have confirmed that surface treatments can significantly reduce the degradation rate of Mg-based materials in chloride-containing solutions. Furthermore, the surface biocompatibility of Mg can also be enhanced using bioactive coatings, such as calcium phosphate coatings [18-20].

Among them, hydroxyapatite (HA) coatings are well recognized because of their excellent bioactivity, which improves the bonding between the metal implant and the bone [21-24].

Hydroxyapatite has hexagonal crystal structure with $Ca_5(PO_4)_3(OH)$ formula. Hydroxyapatite is a ceramic known as bone mineral and is usually in white color. It has many applications areas such as dentistry, skeletal surgery and improving surface hardness of other ceramics. The main reasons for using hydroxyapatite in the surface coating of bio alloys are its porous structure along with its bioactivity and osteointegrity properties [25-27].

In order to improve corrosion resistance of Mg, effect of alloying and HA coating was investigated in this study.

Materials and Methods

In this work, the suitability of alternative materials in place of conventional materials for hard tissue replacement procedures was determined. For this purpose,

Ashby Charts were examined in this study. During the process of preparing these charts, cortical screws and plates properties were considered. It is important that the implant material shows comparable properties to the human bone. The properties of the human bone are given in Table 1.

The charts were drawn according to the data in Table 1. The evaluation of the charts is given in Table 2.

According to Table 2, the most suitable material families are Ti-alloys, stainless steels, and Mg-alloys. Even if most of the properties of Mg is very close to the properties of human bone, its corrosion resistance is very low. In the works of Chen et. al. and Chiu et. al., the low corrosion resistance of Mg made it possible for them to use Mg as a biodegradable material. When examined closer, AZ and WE series Mg alloys are suitable.

The corrosion rate of AZ31 and AZ91 Mg-alloys were examined in this work. To increase the corrosion resistance of these alloys, HA, a naturally occurring compound in the human bone, was used as the coating material.

The Mg-alloys used in this work were supplied by Luoyang Magnesium Gurnee Metal Material Co., Ltd. The chemical compositions of these materials were analyzed by EDS technique and the results are given in Table 3. Mg-alloys used as the backing material in the experiments were cut to the dimensions $50 \times 10 \times 2$ mm and the coating was done on the cut Mg plates.

The coating material in these experiments is HA at 99% purity. The HA was supplied by Xi'an Realin Biotechnology Co.,Ltd. The impurities in the material are given in Table 2. The experiments are designed according to Fig. 1.

Table 1. The Physical and Mechanical Properties of Human Bone [19]

Material	Density (g/cm^3)	Young Modulus (GPa)	Compressive yield strength (MPa)	Fracture Toughness ($MPa.m^{1/2}$)
Naturel Bone	1.8-2.1	3.0 - 20.0	130-180	3-6

Plasma spray coating

Alloys were coated with Atmospheric Plasma Spray Method with HA. The instrument used for this process was Sulzer Metco 9MB plasma gun attached with 730C nozzle. The 16 pads were connected to the turntable and rotated at a rotation speed of 40 rpm. During the rotation HA powder was sprayed. The spray gun was moved up and down with the help of a CNC while the turntables were rotating to ensure that the coating was done homogenously. The total coating time of a specimen of the alloy was set as 3 min. Heat treatment was done on the coated specimens. The heat treatment procedure was done after the accumulation of the coating material on specimen surface. During the heat treatment the

Table 3. AZ31 and AZ91 alloys EDS Results.

	Mg	Al	Zn
AZ31	96,54	2,49	0,96
AZ91	91,32	7,69	0,99

Table 4. HA Chemical Properties.

Sulphate, %	Chloride, %	Heavy metals
<0,048	<0,05	<10(ppm)

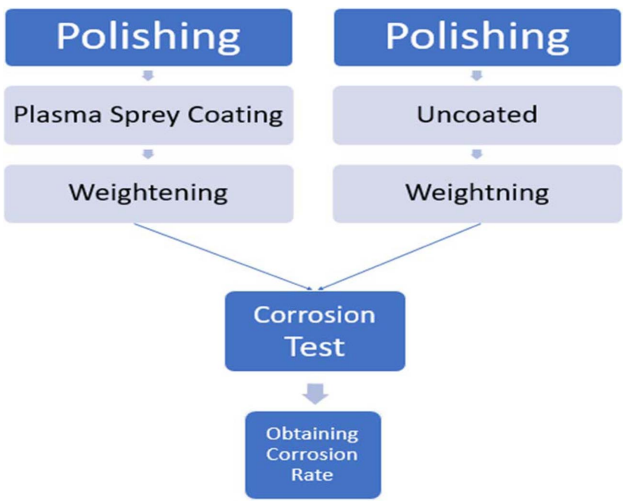

Fig. 1. Flowchart of the experiments.

Table 2 Best options for replacing human bone according to Ashby charts.

Modulus/density	Strength/density	Modulus/strength	Specific modulus/ specific strength	Fracture toughness/ modulus	Fracture toughness/ strength
Steels		Steels	Steels	Steels	Steels
Ti Alloys	Ti Alloys	Ti Alloys	Ti Alloys	Ti Alloys	Ti Alloys
Mg Alloys	Mg Alloys	Mg Alloys	Mg Alloys	Mg Alloys	Mg Alloys
Ni Alloys	SiC	W Alloys	CFRP	Cu Alloys	Ni Alloys
Cu Alloys	CFRP	Cu Alloys	Al Alloys	Al Alloys	Cast Iron
Al Alloys	Si_3N_4	CFRP	Cast Iron	W Alloys	W Alloys
WC		Zn Alloys	Wood	Cast Iron	Cu Alloys
W Alloys		Cast Iron		Zn Alloys	Zn Alloys
Zn Alloys				Ni Alloys	

furnace chamber temperature was increased by 2 degrees Celsius/min to 320 degrees Celsius and the chamber temperature was held constant for 2 h after reaching 320 degrees Celsius. After 2 h the specimens were left to cool down to room temperature.

Corrosion test

Corrosion tests have been started after plasma spray coating. Process has been performed by ASTM G31-72 Standard Practice for Laboratory Immersion Corrosion Testing of Metals. Due to this standard obtained weight lost values converted to average corrosion rate.

$$\text{Corrosion Rate} = (K \times W)/(A \times T \times D) \quad (1)$$

K = a constant
T = time of exposure in hour
A = area in cm^2
W = Weight loss in g
D = density in g/cm^3
K is 8.76×10^4 millimetres per year (mm/y)

Characterization of samples

In this study XRD, SEM and Stereo Microscopy techniques were used for characterization. X-ray diffraction (XRD) analysis was done with Bruker™ D8 Advanced Series powder diffractometer (35 kV and 40 mA) with CuKα (k = 1.5406) radiation at 2 h range of 10-90 using a step size of 0.02 and a rate of 4/min was used for investigations of the HA powder. X'pert High Score software was used for examining HA powder. ZEISS GeminiSEM 500 was used for microstructural analyses both for uncoated alloys and coated alloys. Also, energy dispersive spectrometer (EDS) used for chemical analyses of alloys. YAMER SMT-3020T Trinocular Stereo Zoom Microscope was used to measure coating thickness.

Results and Discussion

During experiments AZ31 and AZ91 alloys were coated hydroxyapatite with plasma spray technique. Then corrosion behavior of alloys was investigated. Before the experiments uncoated AZ31and AZ91 alloys' microstructures were examined and results were given in Fig. 2.

According to Fig. 2 surface areas are clean. Slight scratches from grinding were detected at both surfaces; fortunately, these scratches will be useful for holding the coating. Fig. 3 shows the XRD analysis of HA used in the coating experiments. According to Fig. 3, HA does not contain any impurity.

After the alloys are coated with HA, the characterizations steps of the coatings were started. At different magnifications SEM images of coated AZ31 alloys are given in Fig. 4 and SEM images of coated AZ91 alloys are given in Fig. 5.

When Fig. 4 and Fig. 5 are examined, it is determined

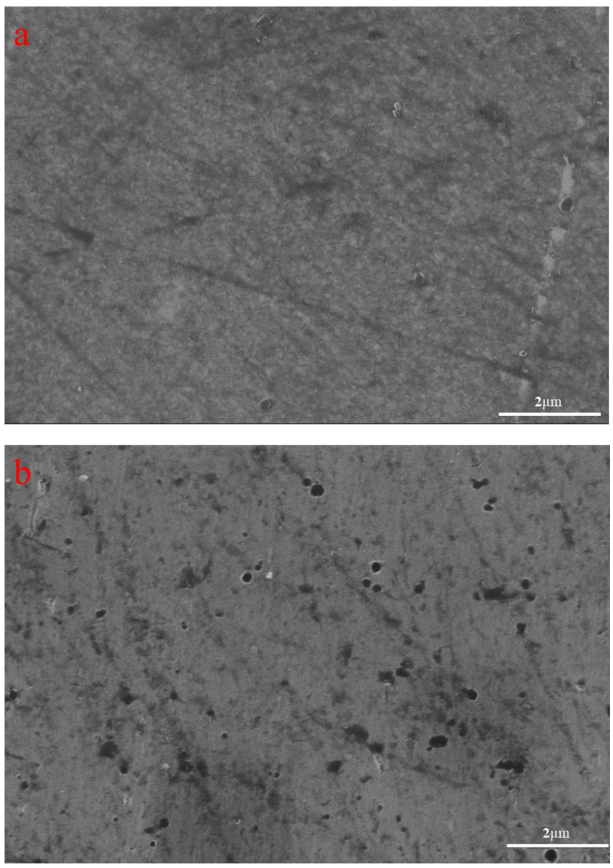

Fig. 2. SEM images of uncoated alloys: (a) AZ91(Mag 20k X). (b) AZ31 (Mag 20k X).

that HA particles are successfully attached to the alloys. According to the images of figures a and b in magnification, the coating was obtained continuously and porously. When the morphology of the coating is examined, there are structures in both spherical and needle form.

After the AZ31 and AZ91 alloys coating morphology were determined, samples were broken vertically to understand the coating thickness. Then measurements were made on Stereo microscope images. In Fig. 6, coating thickness of AZ31 and AZ91 alloys are given.

According to Fig. 6 average coating thickness is over 120 µm for both AZ31 and AZ91. HA coating thicknesses were encountered in literature and the results shows that it changes between 100 nm and 150 µm [28].

In the first stage of the study, coating experiments were made, and surface morphologies were determined by SEM method. In the second stage, corrosion performances were investigated by weight loss method. The weight losses and corrosion rates obtained during the corrosion test are given in Table 5. Corrosion rate for pure magnesium is shown in the literature as approximately 2 mm/y [29]. This rate is determined as 1.2 mm/y for uncoated AZ31 and AZ91 alloys. As a result of HA coating with plasma spray coating, corrosion rate reduced to 0.4 mm/y. In the literature,

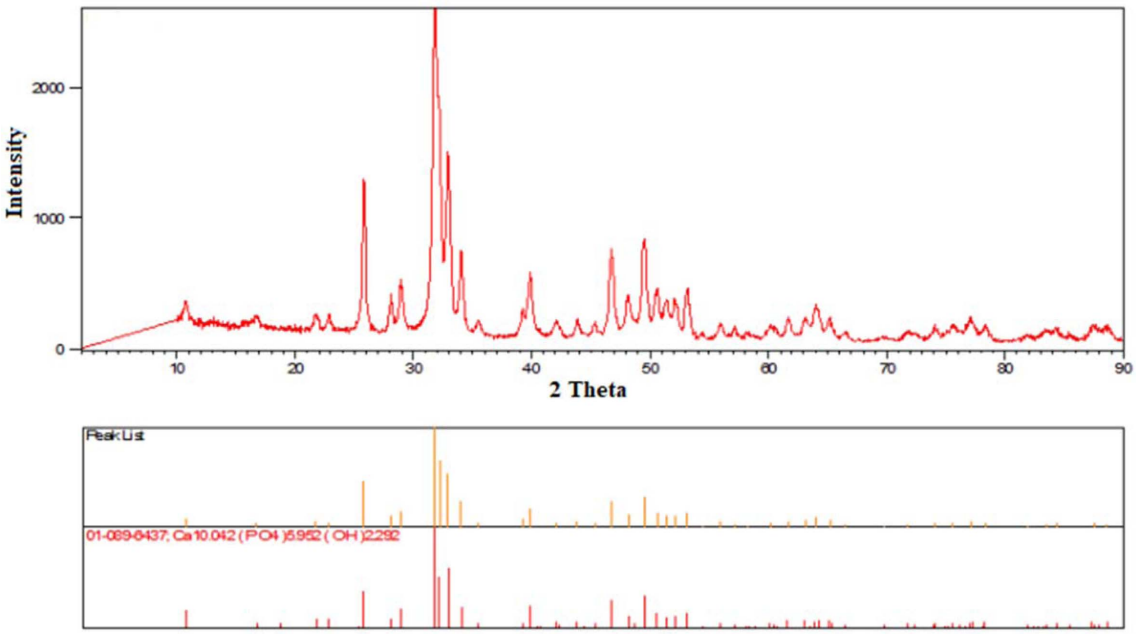

Fig. 3. XRD results of HA.

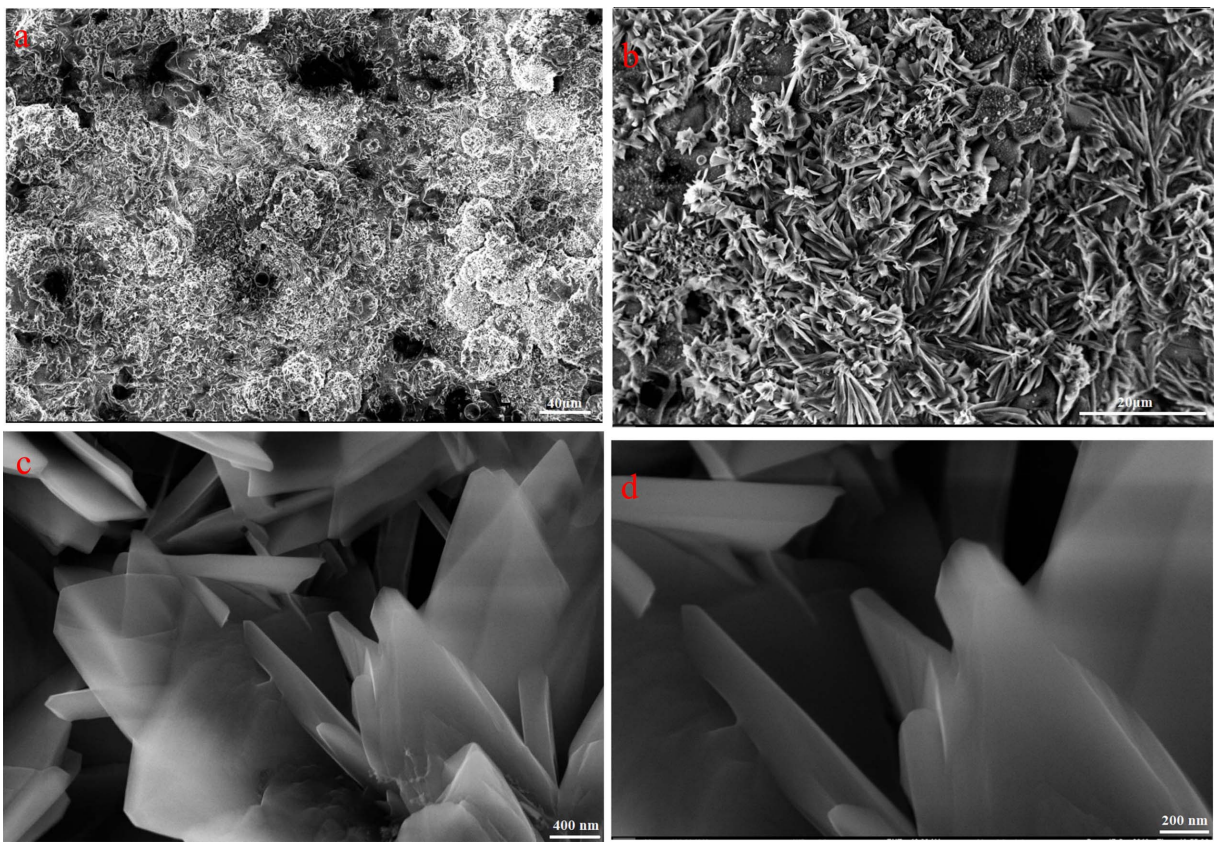

Fig. 4. HA coated microstructure of AZ31 alloy: (a) 500X, (b) 2500X, (c) 50k X, (d) 100k X.

this ratio has been reduced to 0.3 mm/y to 1 mm/y with coating.

In corrosion tests, samples were kept in simulated body fluid at 37.5ºC, for 1, 24 168 and 504 h, weight loss values are given in Fig. 7 for AZ91 and Fig. 8 for AZ31. According to Fig. 7, weight loss determined as 123.1 mg after 504 h was measured as 38.8 mg after coating. Accordingly, the coating improved the corrosion protection potential of the material 3.1 times. Similar findings apply to Fig. 8. Here, the corrosion behaviors

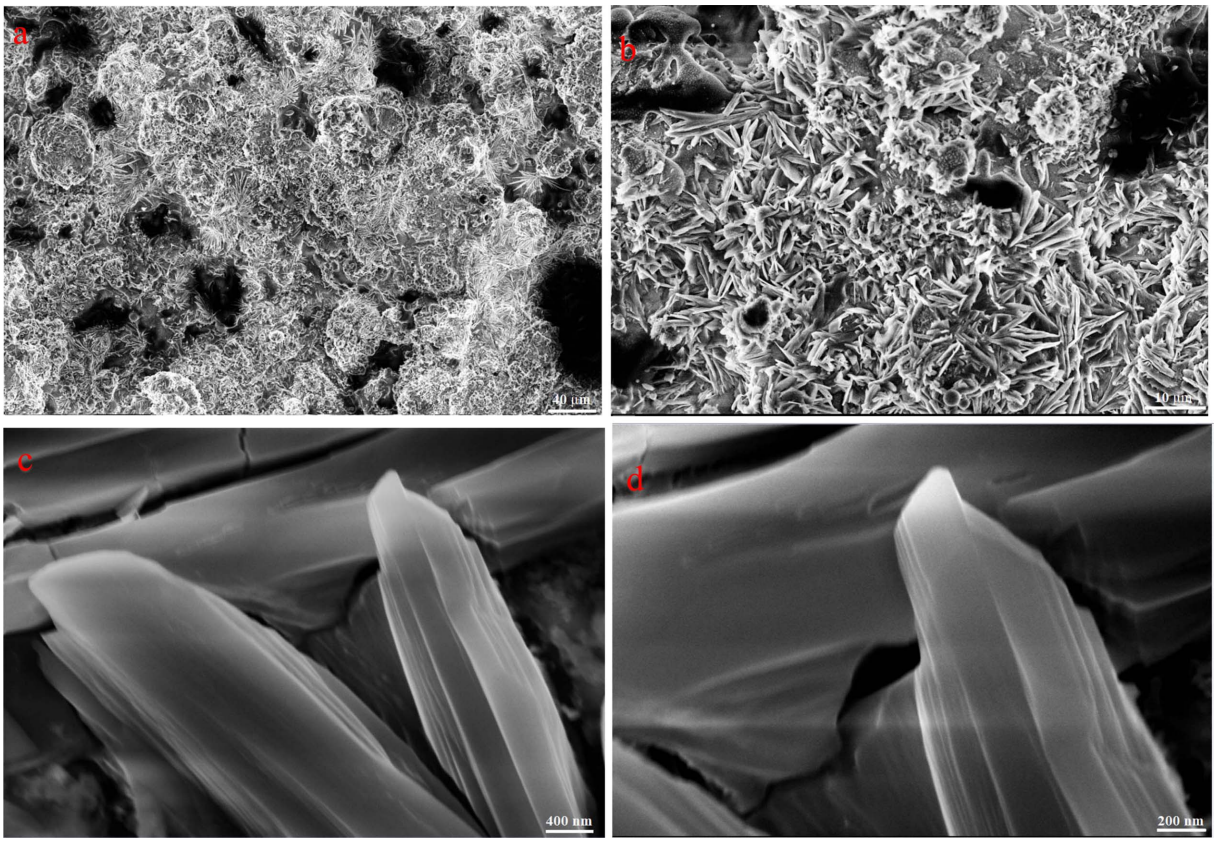

Fig. 5. HA coating microstructure of AZ91 alloy with plasma spray: (a) 500X, (b) 2500X, (c) 50k X, (d) 100k X.

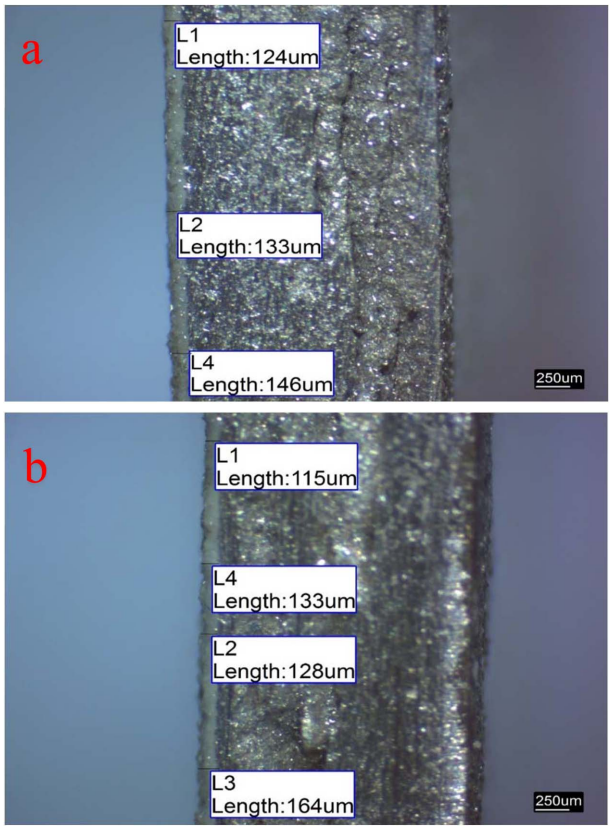

Fig. 6. Coating thicknesses: (a) AZ31, (b) AZ91.

Table 5. Weight losses and corrosion rates during the corrosion test

Time (Hour)	Coating	Alloy	Weight loss (mg)	Corrosion Rate (mm/y)
1	x	AZ31	0,8	3,8640
1	✓	AZ31	0,1	0,4830
1	x	AZ91	0,8	3,7567
1	✓	AZ91	0,1	0,4695
24	x	AZ31	7,1	1,4288
24	✓	AZ31	2,7	0,5433
24	x	AZ91	7,1	1,3892
24	✓	AZ91	2,8	0,5478
168	x	AZ31	47,8	1,3742
168	✓	AZ31	14,3	0,4111
168	x	AZ91	47	1,3137
168	✓	AZ91	13,8	0,3857
504	x	AZ31	127	1,2170
504	✓	AZ31	39,2	0,3756
504	x	AZ91	123,1	1,1469
504	✓	AZ91	38,8	0,3615

of the AZ31 alloy 1, 24 168 and 504 h were examined, and after 504 min the weight loss decreased from 127 mg to 37.2 mg as a result.

After examining the effects of coating on weight loss in the alloys AZ31 and AZ91, the corrosion behavior

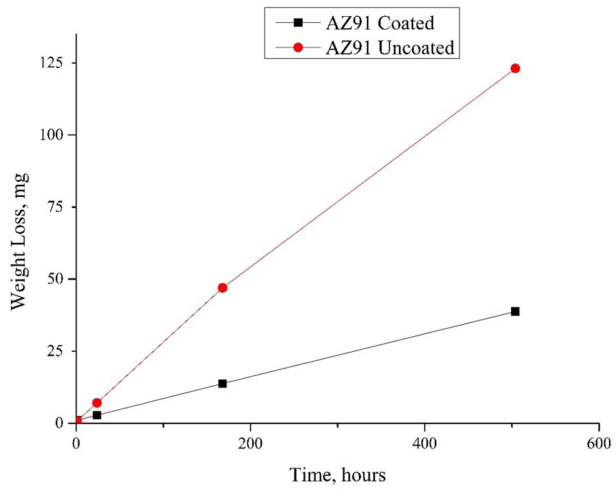

Fig. 7. AZ91 corrosion experiments weight loss results.

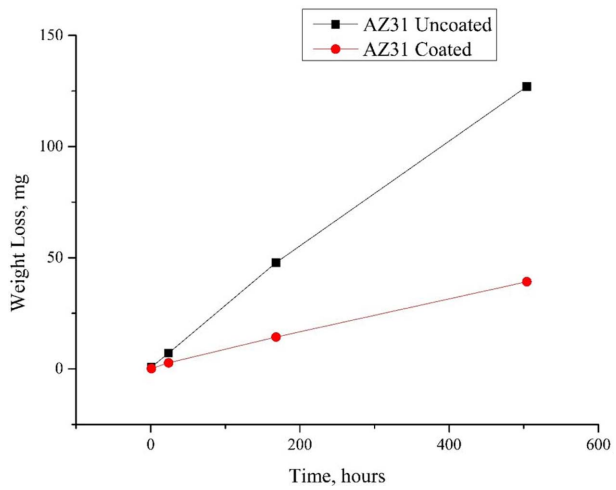

Fig. 8. AZ31 corrosion experiments weight loss results.

of the two alloys was compared with each other, the findings are given in Figure 9. Accordingly, at the end of 504 hours, a weight loss of 127 mg was observed in the alloy of AZ31, while the same conditions were 123.1mg for AZ91. Corrosion behavior of the materials showed similar changes in the graph, it was observed that AZ91 provides better protection with a slight difference compared to AZ31.

The corrosion rates of the samples were calculated by determining the weight losses in the corrosion experiments and replacing the values obtained here with Eq. (1). Fig. 10 shows the corrosion rate of uncoated AZ31 and AZ91 alloys. Accordingly, the materials showed similar corrosion behavior. The corrosion rate, which increased exponentially in the first 1 h, had a horizontal course after 24 h, 1.21 mm/y for AZ31 and 1.14 mm/y for AZ91 after 504 h.

Corrosion rates were determined for uncoated samples as well as HA coated samples, the results are given in Fig. 11 for AZ31 alloy and Fig. 12 for AZ91

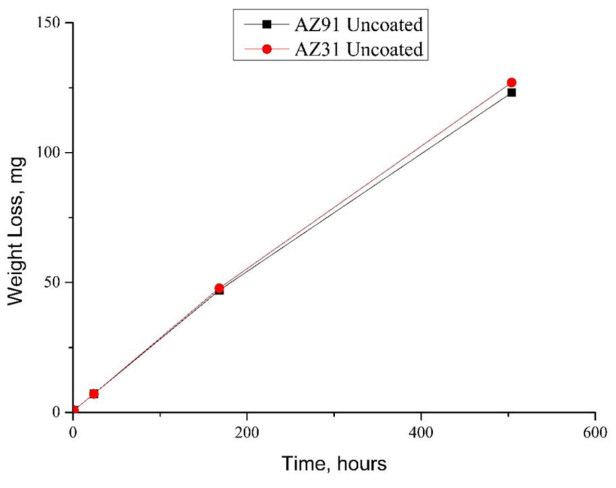

Fig. 9. Uncoated alloys corrosion test weight loss results.

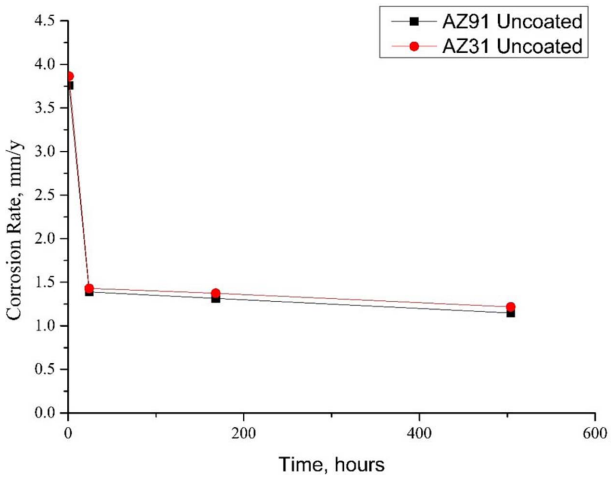

Fig. 10. Uncoated alloys corrosion test corrosion rate results.

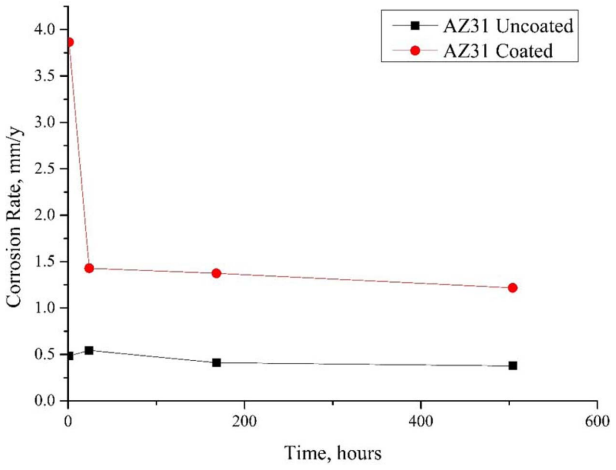

Fig. 11. AZ31 corrosion experiments corrosion rate results.

alloy. It is seen from both graphs that the coating prevents the exponential change that occurs after 1 h in the uncoated sample and protects the sample with a constant corrosion rate. The corrosion rate obtained

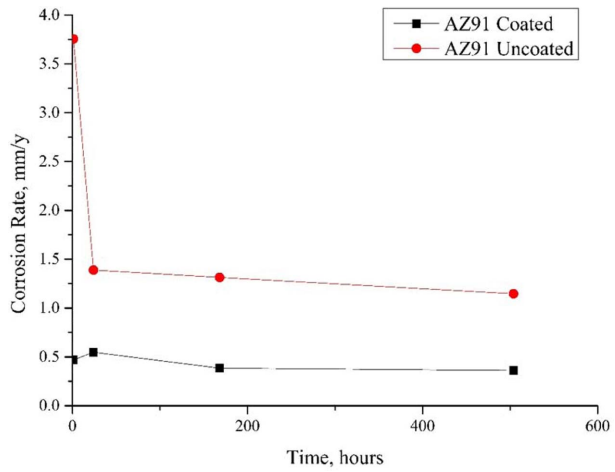

Fig. 12. AZ91 corrosion experiments corrosion rate results.

with a value of 3.86 mm/y after 1 h in Fig. 11 was determined as 0.48 mm/y in the coated sample. In Fig. 12, where the corrosion behavior of AZ91 is examined, the corrosion rate of 3.75 mm/y in the uncoated sample decreased to 0.46 mm/y in the coated sample at the end of 1 h.

Conclusion

In this study, materials that may be alternative to biodegradable implant materials were examined, and as a result of the findings obtained from Ashby Charts, studies were carried out to improve the corrosion behavior of Mg metal. Accordingly, AZ31 and AZ91 Mg alloys were used instead of metallic Mg, and the effects of alloying elements on corrosion behavior were determined. Afterward, the samples were HA coated by the plasma spray method, and the effect of the coating on the corrosion rate was determined by the experiments. When the test results were examined, a high-speed corrosion rate was observed in the uncoated samples at the end of the first 1 h, and then the corrosion rate continued in a horizontal course. For example, the corrosion rate of 3.75 mm/y in AZ91 alloy decreased to 1.38 mm/y at the end of 24 h and then continued at similar values for up to 504 h. When the same sample coated with HA, it was seen that after 1 h, 8.1 times better protection was provided. In addition, the value of 1.38 mm/y obtained at the end of 24 h in which the corrosion rate slowed in the uncoated sample was seen as 0.5 mm/y in the coated sample, and the coating provided 2.76 times better protection even at the lower corrosion rate. In addition, the corrosion prevention capability of AZ31 and AZ91 alloys in the study were examined, and AZ91 was found to be a slightly better corrosion inhibitor even if very close values were obtained. When the data obtained at the end of 504 h are compared in Fig. 10, the corrosion rate, which was 1.21 mm/y for AZ31, was determined as 1.14 mm/y for AZ91.

References

1. K. Hagihara, K. Fujii, A. Matsugaki, and T. Nakano, Mater. Sci. Eng. C 33[7] (2013) 4101-4111.
2. Y. Wang, M. Wei, and J. Gao, Mater. Sci. Eng. C 29[4] (2009) 1311-1316.
3. F. Witte, J. Fischer, J. Nellesen, H.-A. Crostack, V. Kaese, A. Pisch, F. Beckmann, and H. Windhagen, Biomaterials 27[7] (2006) 1013-1018.
4. M.P. Staiger and A.M. Pietak, J. Huadmai, and G. Dias 27[9] (2006) 1728-1734.
5. M. B. Kannan and R. K. S. Raman, Biomaterials 29[15] (2008) 2306-2314.
6. M. Schinhammer, A.C. Hänzi, J.F. Löffler, and P.J. Uggowitzer, Acta Biomater. 6[5] (2010) 1705-1713.
7. M. Mumjitha and V. Raj, J. Mech. Behav. Biomed. Mater. 46[1] (2015) 205-221.
8. X. Gu, Y. Zheng, Y. Cheng, S. Zhong, and T. Xi, Biomaterials, 30[4] (2009) 484-498.
9. H. Hermawan, H. Alamdari, D. Mantovani, and D. Dub, Powder Metall. 51[1] (2008) 38-45.
10. Z. Li, X. Gu, S. Lou, and Y. Zheng, Biomaterials, 29[10] (2008) 1329-1344.
11. G.L. Zhao, L. Xia, B. Zhong, S.S. Wu, L. Song, and G.W. Wen, Trans. Nonferrous Met. Soc. China 25[4] (2015) 1151-1157.
12. J.H. Jo, B.G. Kang, K.S. Shin, H.E. Kim, B.D. Hahn, D.S. Park, and Y.H. Koh, J. Mater. Sci. Mater. Med. 22[11] (2011) 2437-2447.
13. S.Z. Khalajabadi, M.R. Abdul Kadir, S. Izman, and R. Ebrahimi-Kahrizsangi, Mater. Des. 88[1] (2015) 1223-1233.
14. Y. Chen, Z. Xu, C. Smith, and J. Sankar, Acta Biomater. 10[11] (2014) 4561-4573.
15. H.Y. Choi and W.J. Kim, J. Mech. Behav. Biomed. Mater. 51[1] (2015) 291-301.
16. K.Y. Chiu, M.H. Wong, F.T. Cheng, and H.C. Man, Surf. Coatings Technol. 202[3] (2007) 590-598.
17. G. Song and S. Song, Adv. Eng. Mater., 9[4] (2007) 298-302.
18. C. Wen, S. Guan, L. Peng, C. Ren, X. Wang, and Z. Hu, Appl. Surf. Sci., 255[13] (2009) 6433-6438.
19. Y. Zhang, G. Zhang, and M. Wei, J. Biomed. Mater. Res. B 89[2] (2009) 408-414.
20. L. Xu, F. Pan, G. Yu, L. Yang, E. Zhang, and K. Yang, Biomaterials 30[8] (2009) 1512-1523.
21. D. Lakstein, W. Kopelovitch, Z. Barkay, M. Bahaa, D. Hendel, and N. Eliaz, Acta Biomater. 5[6] (2009) 2258-2269.
22. A. Bigi, M. Fini, B. Bracci, E. Boanini, P. Torricelli, G. Giavaresi, N.N. Aldini, A. Facchini, F. Sbaiz, and R. Giardino, Biomaterials 29[11] (2008) 1730-1736.
23. M. Yetmez, Z.E. Erkmen, C. Kalkandelen, A. Ficai, and F.N. Oktar, Mater. Sci. Eng. C 77[1] (2017) 470-475.
24. S. Pazarlioglu and S. Salman, J. Ceram. Process. Res. 20[1] (2019) 99-112.
25. X. Yue, L. Xu, Q. Tian, L. Feng, and K. Sun, J. Ceram. Process. Res. 18[7] (2017) 531-535.
26. J.H. Lim, C.K. Park, C.H. Jin, S.Y. Beck, and D.Y. Jeong, J. Ceram. Process. Res. 18[5] (2017) 404-408.
27. E. Nazmi, J. Ceram. Process. Res. 18[1] (2017) 64-68.
28. G. Lewis, J. Adv. Nanomater. 2[1] (2017) 65-82.
29. X.B. Chen, N. Birbilis, and T.B. Abbott, Corros. Sci. 53[6] (2011) 2263-2268.